

Supporting information for

Spatially Extended Asymmetry Directs Electron Transfer and Modulates Water

Oxidation Deprotonation Behavior on Dual-Atom Catalysts

Jixuan Yang, †^{a,b} Yaxin Cheng, †^{b,c} Hao Ma, †^d Zirui Wang, ^b Ting Wang^c and Yuanmiao Sun^{b*}

^a *Southern University of Science and Technology, Shenzhen, Guangdong 518055, China*

^b *Institute of Technology for Carbon Neutrality, Shenzhen Institutes of Advanced Technology, Chinese Academy of Sciences, Shenzhen, 518055, China*

^c *College of the Environment & Ecology, Fujian Key Laboratory of Coastal Pollution Prevention and Control, Xiamen University, Xiamen 361102, P.R. China*

^d *School of Information and Electronic Engineering, Shandong Technology and Business University, Yantai, 264005, China*

†These authors contributed equally to this work.

*Corresponding authors. Email: sunym@siat.ac.cn

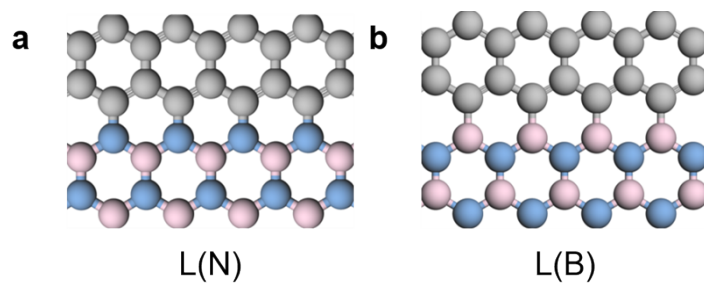


Fig S1. Schematic structures of the h-BN/Gra heterostructures with two types of interfacial connections.

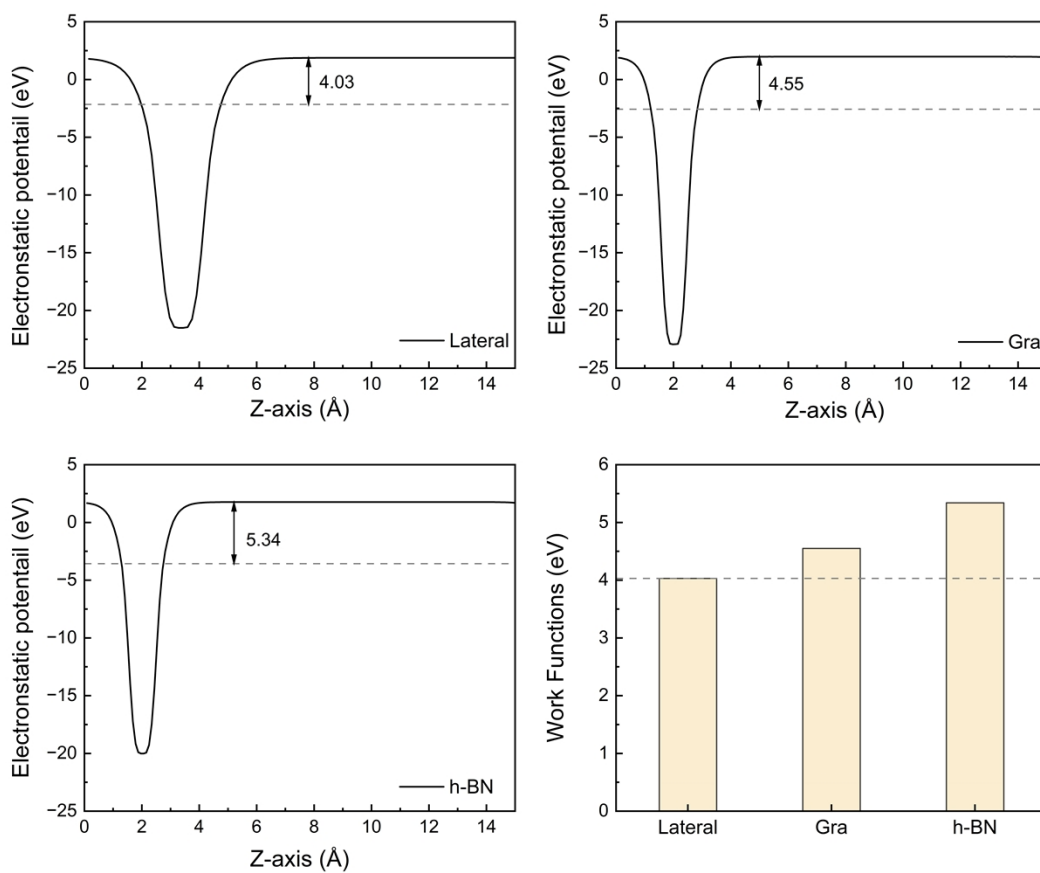


Fig S2. Work functions of the h-BN/graphene heterostructure, monolayer h-BN, and graphene.

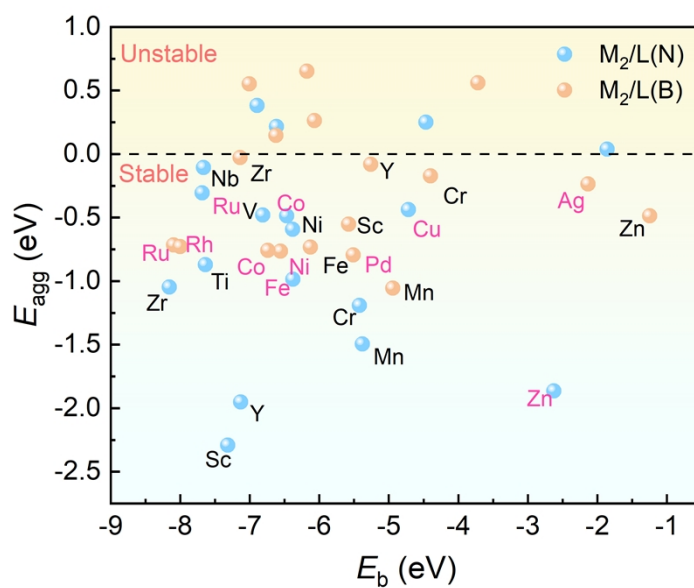


Fig S3. Cohesive and aggregation energies of $M_2/L(N)$ and $M_2/L(B)$ systems. The cohesive energy is calculated as $E_c = E_{bulk} - E_{M(atom)}$, the binding energy as $E_b = E_{2M/sbab} - E_{sbab} - 2E_{M(atom)}$, and the aggregation energy as $E_{agg} = E_b - E_c$.

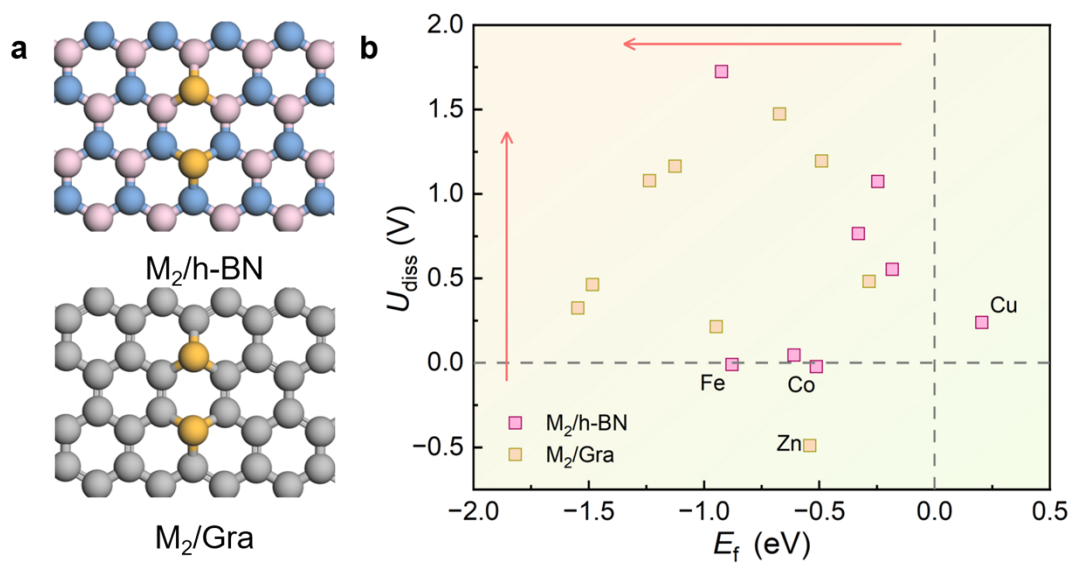


Fig S4. Structural models and stability screening of $M_2/h\text{-BN}$ and M_2/Gra systems. The stability is evaluated based on the formation energy (E_f) and the dissolution potential (U_{diss}).

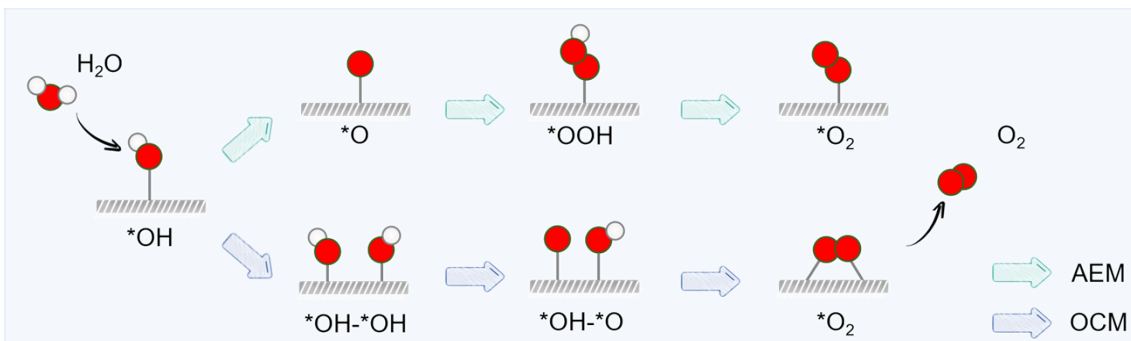


Fig S5. Schematic illustration of the two distinct OER pathways, including the AEM and OCM.

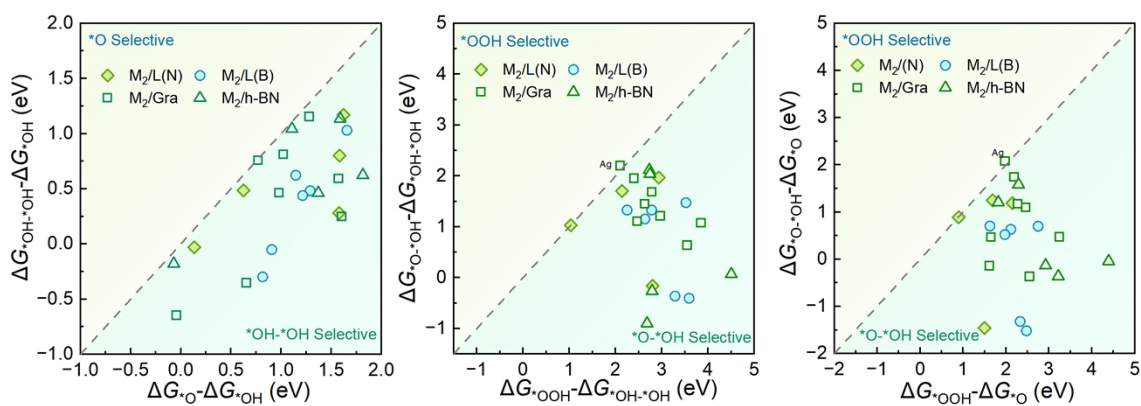


Fig S6. Gibbs free energy changes from *OH to *O versus *OH-*OH, from *O to *OOH versus *O-*OH, and from *OH-*OH to *OOH versus *O-*OH.

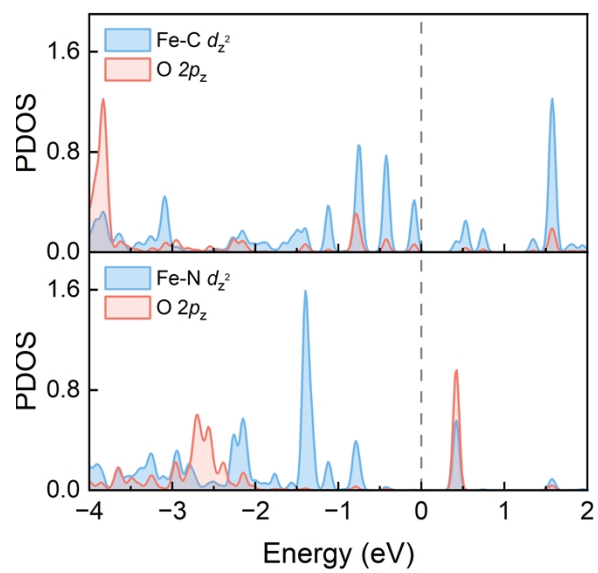


Fig S7. Comparison of the PDOS of the Fe d_z^2 and O $2p_z$ orbitals at the M-C site and the M-N site in $\text{Fe}_2/\text{L}(\text{N})$.

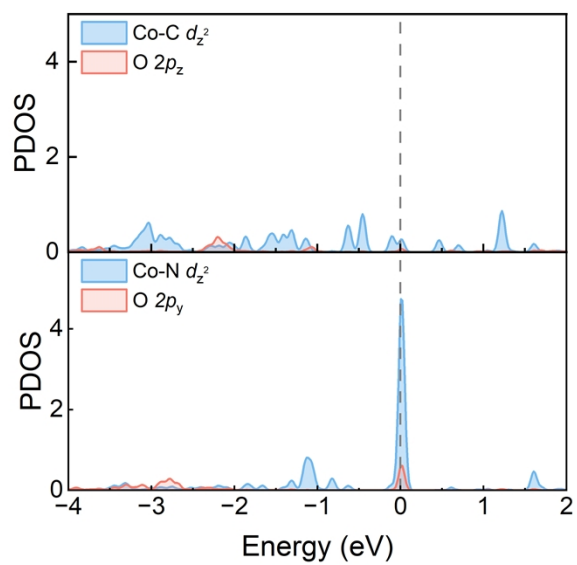


Fig S8. Comparison of the PDOS of the Co d_z^2 and O $2p_z$ orbitals at the M-C site and the M-N site in $\text{Co}_2/\text{L}(\text{N})$.

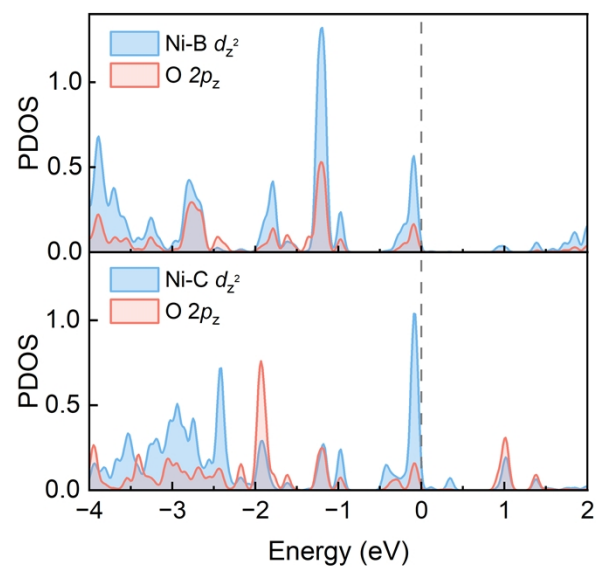


Fig S9. Comparison of the PDOS of the Ni d_z^2 and O $2p_z$ orbitals at the M-B site in and the M-C site in $\text{Ni}_2/\text{L}(\text{B})$.

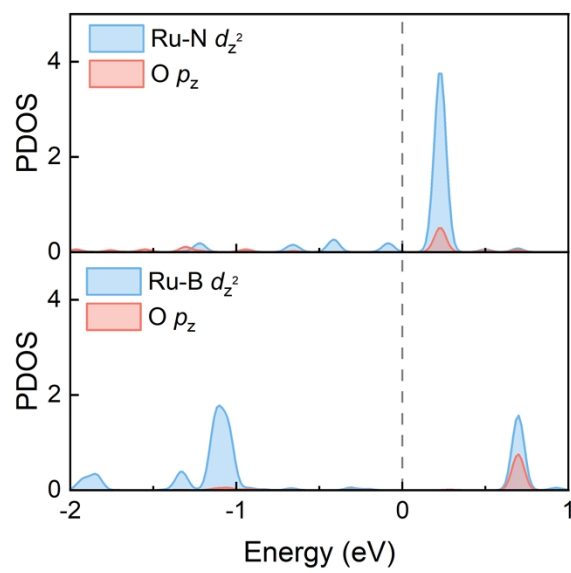


Fig S10. Comparison of the PDOS of the Rh d_z^2 and O $2p_z$ orbitals at the M-N site in Ru₂/L(N) and the M-B site in Ru₂/L(B).

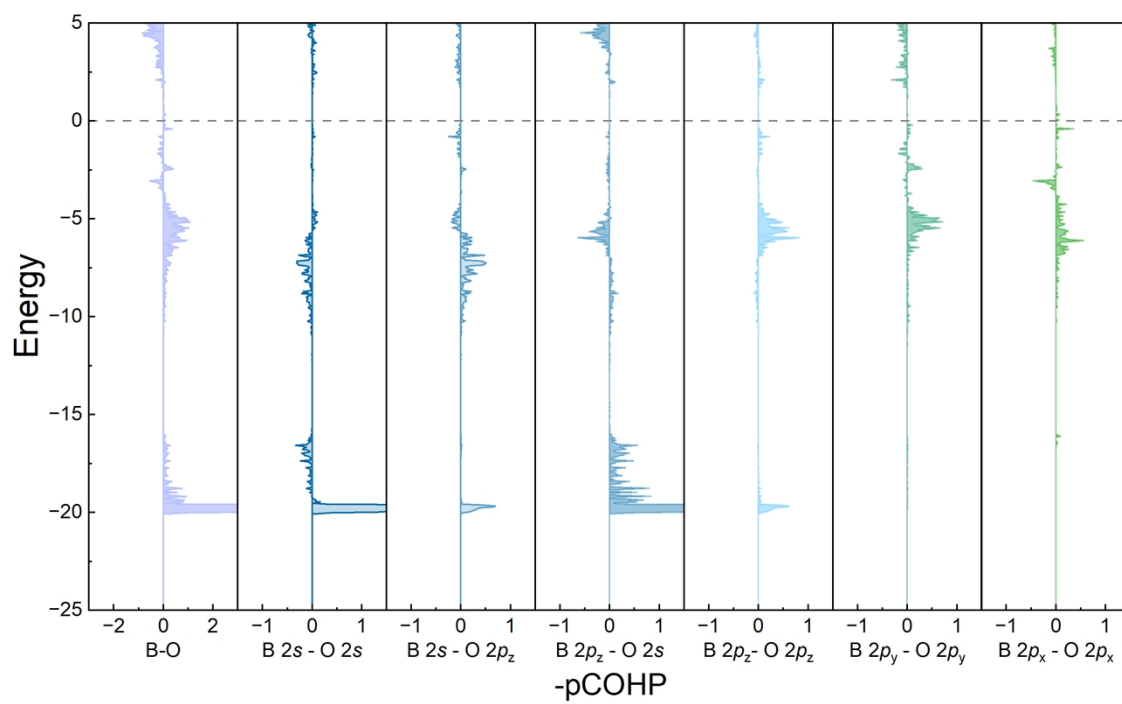


Fig S11. COHP analysis of B-O bonding in the *O-*OH co-adsorption configuration of Ru₂/L(B), decomposed into B(2s) - O(2s), B(2s) - O(2p_z), B(2p_z) - O(2s), B(2p_z) - O(2p_z), B(2p_y) - O(2p_y) and B(2p_x) - O(2p_x) orbital contributions.

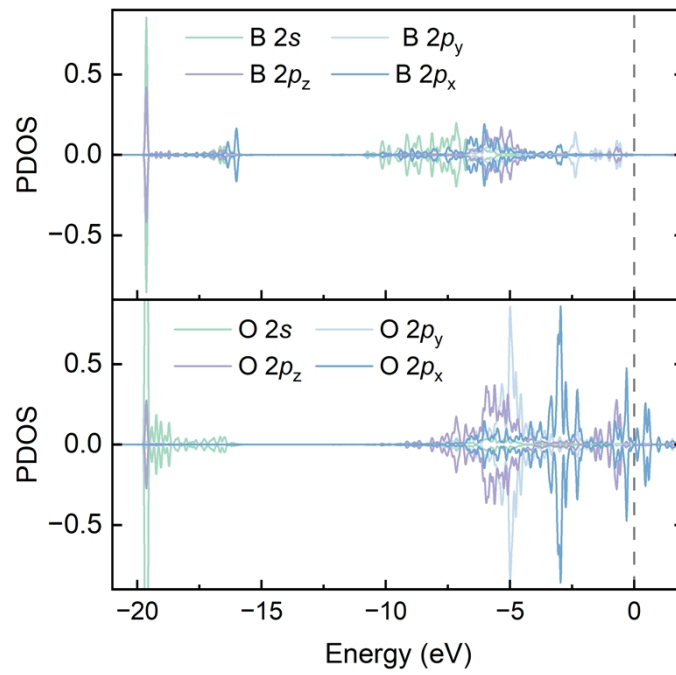


Fig S12. PDOS analysis of B-O bonding in the *O-*OH co-adsorption configuration of Ru₂/L(B).

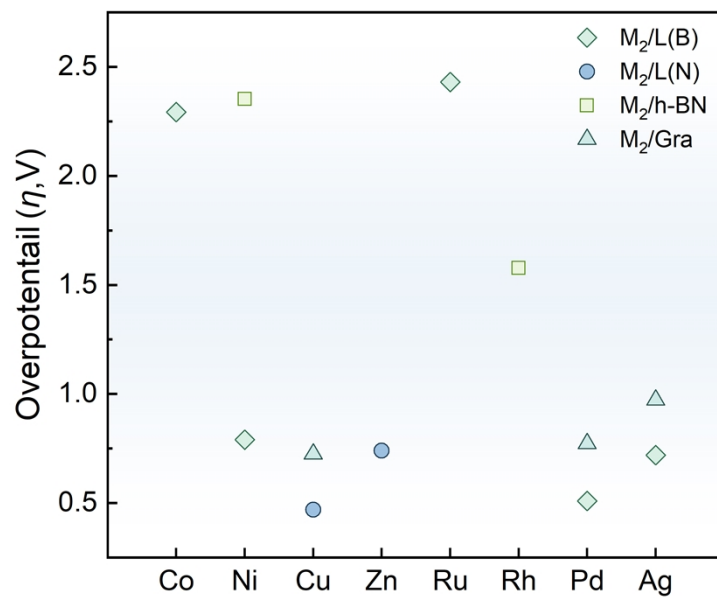


Fig S13. Comparison of the overpotentials of the four investigated DACs systems after excluding those with hindered O_2 desorption.

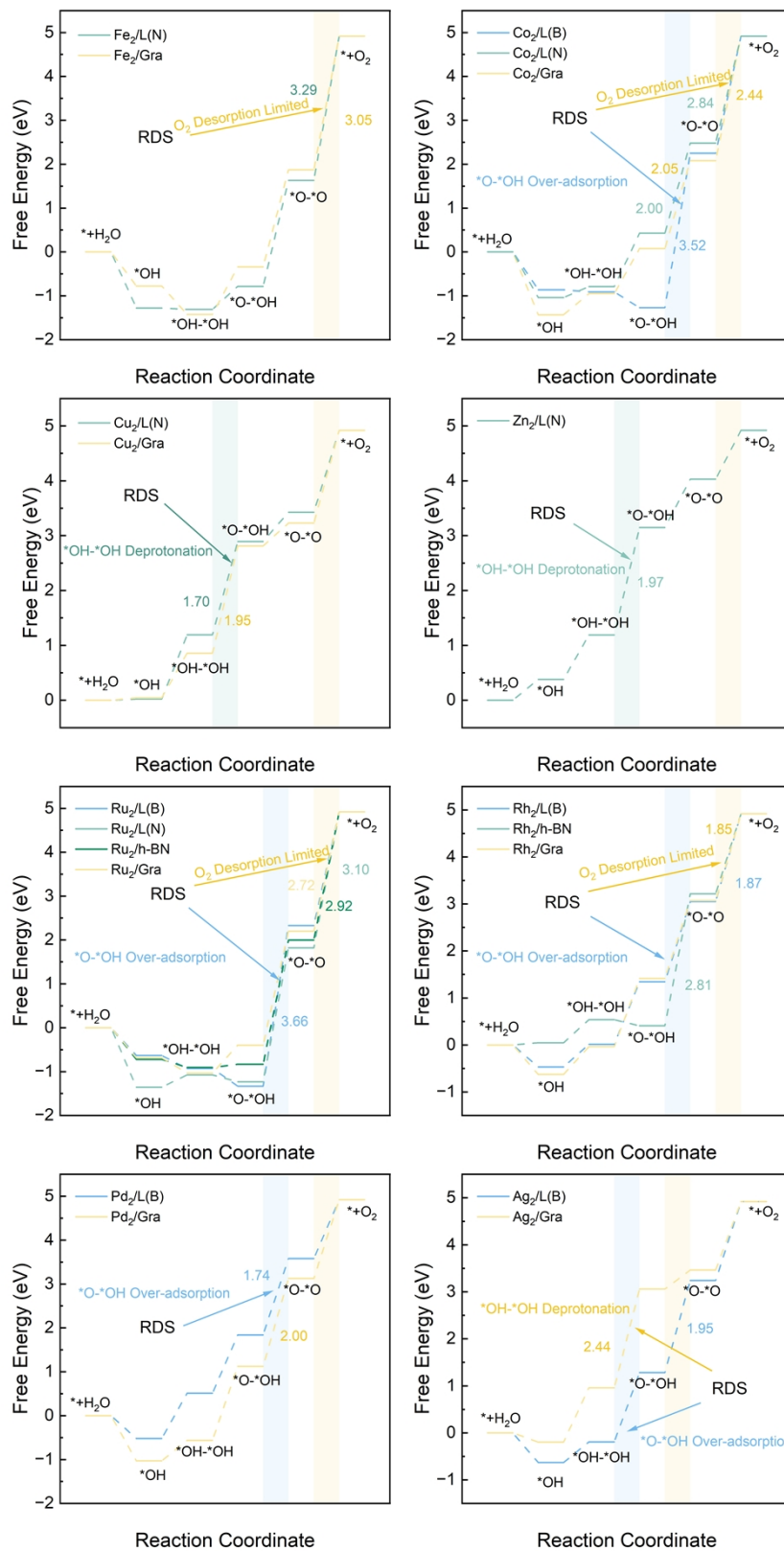


Fig S14. Gibbs free energy diagrams of the OCM reaction pathway at 0 V (vs RHE) for Fe, Co, Cu, Zn, Ru, Rh, Pd, and Ag DACs supported on h-BN/Gra heterostructure, h-BN, and graphene.

Table S1. Computed formation energies (E_f) and dissolution potentials (U_{diss}) of $M_2/L(N)$ and $M_2/L(B)$. Here, U^0 is standard dissolution potentials at pH=0, N_e is number of electrons involved in the dissolution for the pure metals.

Metal	Pattern	$E_{\text{bulk}}(\text{eV/atom})$	$U^0(\text{V})$	N_e	$E_f(\text{eV})$	$U_{\text{diss}}(\text{V vs SHE})$
Sc	L(N)	-6.911	-2.08	3	-2.291	-1.316
	L(B)				-0.552	-1.896
Ti	L(N)	-8.401	-1.63	2	-0.871	-1.195
	L(B)				0.145	-1.703
V	L(N)	-9.855	-1.18	2	-0.481	-0.940
	L(B)				0.263	-1.311
Cr	L(N)	-9.667	-0.91	2	-1.192	-0.314
	L(B)				-0.172	-0.824
Mn	L(N)	-8.994	-1.19	2	-1.494	-0.443
	L(B)				-1.056	-0.662
Fe	L(N)	-8.494	-0.45	2	-0.986	0.043
	L(B)				-0.732	-0.084
Co	L(N)	-7.432	-0.28	2	-0.593	0.017
	L(B)				-0.764	0.102
Ni	L(N)	-5.915	-0.26	2	-0.487	-0.016
	L(B)				-0.758	0.119
Cu	L(N)	-4.523	0.34	2	-0.439	0.559
	L(B)				0.559	0.060
Zn	L(N)	-0.773	-0.76	2	-1.864	0.172
	L(B)				-0.487	-0.516
Y	L(N)	-7.325	-2.37	3	-1.951	-1.720
	L(B)				-0.080	-2.343
Zr	L(N)	-9.036	-1.45	4	-1.048	-1.188
	L(B)				-0.028	-1.443
Nb	L(N)	-10.693	-1.10	3	-0.106	-1.065
	L(B)				0.552	-1.284
Mo	L(N)	-11.419	-0.20	3	0.216	-0.272
	L(B)				0.652	-0.417
Ru	L(N)	-9.618	0.46	2	-0.306	0.613
	L(B)				-0.716	0.818
Rh	L(N)	-7.871	0.60	2	0.382	0.409
	L(B)				-0.729	0.964
Pd	L(N)	-5.849	0.95	2	0.250	0.825
	L(B)				-0.794	1.347
Ag	L(N)	-3.162	0.80	1	0.038	0.762
	L(B)				-0.236	1.036

Table S2. Comparison of the formation energies (E_f) and dissolution potentials (U_{diss}) for 11 thermodynamically and electrochemically stable M_2 /Lateral heterostructure with corresponding M_2 /h-BN and M_2 /Gra systems.

Metal	Pattern	$E_{\text{bulk}}(\text{eV/atom})$	$U^0(\text{V})$	N_e	$E_f(\text{eV})$	$U_{\text{diss}}(\text{V vs SHE})$
Fe	L(N)	-8.494	-0.45	2	-0.986	0.043
	L(B)				-0.732	-0.084
	h-BN				-0.878	-0.011
	Gra				-1.547	0.324
Co	L(N)	-7.432	-0.28	2	-0.593	0.017
	L(B)				-0.764	0.102
	h-BN				-0.513	-0.024
	Gra				-1.483	0.462
Ni	L(N)	-5.915	-0.26	2	-0.487	-0.016
	L(B)				-0.758	0.119
	h-BN				-0.610	0.045
	Gra				-0.946	0.213
Cu	L(N)	-4.523	0.34	2	-0.439	0.559
	L(B)				0.559	0.060
	h-BN				0.205	0.237
	Gra				-0.283	0.482
Zn	L(N)	-0.773	-0.76	2	-1.864	0.172
	L(B)				-0.487	-0.516
	h-BN				-1.765	0.123
	Gra				-	-
Ru	L(N)	-9.618	0.46	2	-0.306	0.613
	L(B)				-0.716	0.818
	h-BN				-0.184	0.552
	Gra				-1.236	1.078
Rh	L(N)	-7.871	0.60	2	0.382	0.409
	L(B)				-0.729	0.964
	h-BN				-0.330	0.765
	Gra				-1.125	1.163
Pd	L(N)	-5.849	0.95	2	0.250	0.825
	L(B)				-0.794	1.347
	h-BN				-0.245	1.073
	Gra				-0.489	1.195
Ag	L(N)	-3.162	0.80	1	0.038	0.762
	L(B)				-0.236	1.036
	h-BN				-0.923	1.723
	Gra				-0.672	1.472

Table S3. Total energies (E), free energy corrections of surface-adsorbed molecules [$G(T) = E_{ZPE} + \Delta U - TS$], and Gibbs free energy (ΔG^*) of oxidation intermediates adsorbed on different coordinated metal sites in the $\text{Fe}_2/\text{L}(\text{N})$ system under the AEM and OCM mechanisms.

	Species	E (eV)	$G(T)$ (eV)	ΔG^* (eV)
Fe-N	Slab	-1143.61	0	0
	*OH	-1156.05	0.33	-1.28
	*O	-1152.22	0.06	-1.13
	*OOH	-	-	-
	*OH-*OH	-1167.19	0.60	-1.31
	*O-*OH	-1162.97	0.32	-0.78
	Slab	-1143.61	0	0
Fe-C	*OH	-1156.05	0.33	-1.28
	*O	-1152.23	0.05	-1.14
	*OOH	-	-	-
	*OH-*OH	-1167.19	0.60	-1.31
	*O-*OH	-1162.71	0.40	-0.45

Table S4. Total energies (E), free energy corrections of surface-adsorbed molecules [$G(T) = E_{ZPE} + \Delta U - TS$], and Gibbs free energy (ΔG^*) of oxidation intermediates adsorbed on different coordinated metal sites in the $\text{Co}_2/\text{L}(\text{N})$ system under the AEM and OCM mechanisms.

	Species	E (eV)	$G(T)$ (eV)	ΔG^* (eV)
Co-N	Slab	-1141.20	0	0
	*OH	-1153.80	0.35	-1.41
	*O	-1149.50	0.06	-0.81
	*OOH	-1158.14	0.34	1.67
	*OH-*OH	-1164.48	0.66	-0.95
	*O-*OH	-1159.70	0.32	0.08
Co-C	Slab	-1141.20	0	0
	*OH	-1153.82	0.35	-1.43
	*O	-1149.50	0.06	-0.81
	*OOH	-	-	-
	*OH-*OH	-1164.48	0.66	-0.95
	*O-*OH	-1159.35	0.31	0.43

Table S5. Total energies (E), free energy corrections of surface-adsorbed molecules [$G(T) = E_{ZPE} + \Delta U - TS$], and Gibbs free energy (ΔG^*) of oxidation intermediates adsorbed on different coordinated metal sites in the $\text{Cu}_2/\text{L}(\text{N})$ system under the AEM and OCM mechanisms.

	Species	E (eV)	$G(T)$ (eV)	ΔG^* (eV)
Cu-N	Slab	-1133.99	0	0
	*OH	-1145.15	0.36	0.03
	*O	-1139.84	0.05	1.63
	*OOH	-1149.30	0.36	3.31
	*OH-*OH	-1155.07	0.60	1.19
	*O-*OH	-1149.69	0.33	2.89
Cu-C	Slab	-1133.99	0	0
	*OH	-1145.15	0.35	0.02
	*O	-1139.84	0.06	1.65
	*OOH	-1149.31	0.39	3.33
	*OH-*OH	-1155.07	0.60	1.19
	*O-*OH	-1149.69	0.33	2.89

Table S6. Total energies (E), free energy corrections of surface-adsorbed molecules [$G(T) = E_{ZPE} + \Delta U - TS$], and Gibbs free energy (ΔG^*) of oxidation intermediates adsorbed on different coordinated metal sites in the $Zn_2/L(N)$ system under the AEM and OCM mechanisms.

	Species	E (eV)	$G(T)$ (eV)	ΔG^* (eV)
Zn-N	Slab	-1144.37	0.00	0
	*OH	-1140.71	0.34	0.38
	*O	-1135.43	0.05	1.97
	*OOH	-1144.37	0.30	4.12
	*OH-*OH	-1151.01	0.60	1.19
	*O-*OH	-1145.34	0.31	3.16
Zn-C	Slab	-1144.37	0.00	0
	*OH	-1140.38	0.28	0.66
	*O	-1134.51	0.01	2.86
	*OOH	-1144.59	0.30	3.90
	*OH-*OH	-1151.01	0.60	1.19
	*O-*OH	-1145.34	0.31	3.15

Table S7. Total energies (E), free energy corrections of surface-adsorbed molecules [$G(T) = E_{ZPE} + \Delta U - TS$], and Gibbs free energy (ΔG^*) of oxidation intermediates adsorbed on different coordinated metal sites in the Ru₂/L(N) system under the AEM and OCM mechanisms.

	Species	E (eV)	$G(T)$ (eV)	ΔG^* (eV)
Ru-N	Slab	-1144.49	0	0
	*OH	-1157.05	0.37	-1.35
	*O	-1152.87	0.04	-0.91
	*OOH	-1162.41	0.37	0.72
	*OH-*OH	-1167.79	0.55	-1.07
	*O-*OH	-1164.31	0.32	-1.23
Ru-C	Slab	-1144.49	0	0
	*OH	-1157.05	0.37	-1.35
	*O	-1151.73	0.03	0.22
	*OOH	-1161.40	0.37	1.73
	*OH-*OH	-1167.79	0.55	-1.07
	*O-*OH	-1163.37	0.34	-0.27

Table S8. Total energies (E), free energy corrections of surface-adsorbed molecules [$G(T) = E_{ZPE} + \Delta U - TS$], and Gibbs free energy (ΔG^*) of oxidation intermediates adsorbed on different coordinated metal sites in the $\text{Co}_2/\text{L}(\text{B})$ system under the AEM and OCM mechanisms.

	Species	E (eV)	$G(T)$ (eV)	ΔG^* (eV)
Co-B	Slab	-1137.74	0	0
	*OH	-1149.44	0.28	-0.59
	*O	-1144.42	0.02	0.77
	*OOH	-1153.76	0.32	2.56
	*OH-*OH	-1160.90	0.58	-0.91
	*O-*OH	-1157.71	0.44	-1.27
Co-C	Slab	-1137.74	0	0
	*OH	-1149.76	0.33	-0.86
	*O	-1145.17	0.05	0.05
	*OOH	-1153.95	0.32	2.38
	*OH-*OH	-1160.90	0.58	-0.91
	*O-*OH	-1155.98	0.33	-0.86

Table S9. Total energies (E), free energy corrections of surface-adsorbed molecules [$G(T) = E_{ZPE} + \Delta U - TS$], and Gibbs free energy (ΔG^*) of oxidation intermediates adsorbed on different coordinated metal sites in the Ni₂/L(B) system under the AEM and OCM mechanisms.

		Species	E (eV)	$G(T)$ (eV)	ΔG^* (eV)
Ni-B		Slab	-1134.90	0	0
		*OH	-1146.52	0.23	-0.56
		*O	-1142.03	0.05	0.34
		*OOH	-1150.62	0.32	2.85
		*OH-*OH	-1157.30	0.56	-0.18
		*O-*OH	-1151.76	0.31	1.71
Ni-C		Slab	-1134.90	0	0
		*OH	-1146.87	0.34	-0.80
		*O	-1142.03	0.05	0.34
		*OOH	-1151.04	0.34	2.46
		*OH-*OH	-1157.30	0.56	-0.18
		*O-*OH	-1152.51	0.33	0.98

Table S10. Total energies (E), free energy corrections of surface-adsorbed molecules [$G(T) = E_{\text{ZPE}} + \Delta U - TS$], and Gibbs free energy (ΔG^*) of oxidation intermediates adsorbed on different coordinated metal sites in the Ru₂/L(B) system under the AEM and OCM mechanisms.

	Species	E (eV)	$G(T)$ (eV)	ΔG^* (eV)
Ru-B	Slab	-1141.51	0	0
	*OH	-1152.84	0.27	-0.23
	*O	-1148.80	0.03	0.17
	*OOH	-1157.04	0.29	3.02
	*OH-*OH	-1164.67	0.56	-0.93
	*O-*OH	-1161.47	0.37	-1.33
Ru-C	Slab	-1141.51	0	0
	*OH	-1153.31	0.33	-0.63
	*O	-1148.80	0.04	0.19
	*OOH	-1157.45	0.33	2.66
	*OH-*OH	-1164.67	0.56	-0.93
	*O-*OH	-1159.94	0.30	0.13

Table S11. Total energies (E), free energy corrections of surface-adsorbed molecules [$G(T) = E_{\text{ZPE}} + \Delta U - TS$], and Gibbs free energy (ΔG^*) of oxidation intermediates adsorbed on different coordinated metal sites in the Rh₂/L(B) system under the AEM and OCM mechanisms.

		Species	E (eV)	$G(T)$ (eV)	ΔG^* (eV)
Rh-B		Slab	-1139.40	0	0
		*OH	-1150.61	0.27	-0.11
		*O	-1145.31	0.02	1.54
		*OOH	-1154.93	0.32	3.06
		*OH-*OH	-1161.63	0.58	0.01
		*O-*OH	-1156.09	0.28	1.85
Rh-C		Slab	-1139.40	0	0
		*OH	-1151.01	0.30	-0.47
		*O	-1146.04	0.04	0.82
		*OOH	-1155.21	0.34	2.80
		*OH-*OH	-1161.63	0.58	0.01
		*O-*OH	-1156.65	0.33	1.34

Table S12. Total energies (E), free energy corrections of surface-adsorbed molecules [$G(T) = E_{\text{ZPE}} + \Delta U - TS$], and Gibbs free energy (ΔG^*) of oxidation intermediates adsorbed on different coordinated metal sites in the Pd₂/L(B) system under the AEM and OCM mechanisms.

	Species	E (eV)	$G(T)$ (eV)	ΔG^* (eV)
Pd-B	Slab	-1134.82	0	0
	*OH	-1146.50	0.32	-0.52
	*O	-1141.15	0.04	1.14
	*OOH	-1150.65	0.34	2.78
	*OH-*OH	-1156.56	0.58	0.51
	*O-*OH	-1150.64	0.31	2.75
Pd-C	Slab	-1134.82	0	0
	*OH	-1146.50	0.32	-0.52
	*O	-1141.15	0.04	1.14
	*OOH	-1150.65	0.32	2.76
	*OH-*OH	-1156.56	0.58	0.51
	*O-*OH	-1151.56	0.31	1.84

Table S13. Total energies (E), free energy corrections of surface-adsorbed molecules [$G(T) = E_{\text{ZPE}} + \Delta U - TS$], and Gibbs free energy (ΔG^*) of oxidation intermediates adsorbed on different coordinated metal sites in the $\text{Ag}_2/\text{L}(\text{B})$ system under the AEM and OCM mechanisms.

		Species	E (eV)	$G(T)$ (eV)	ΔG (eV)
Ag-B		Slab	-1125.52	0	0
		*OH	-1137.31	0.33	-0.63
		*O	-1132.41	0.05	0.58
		*OOH	-1140.76	0.31	3.33
		*OH-*OH	-1147.96	0.59	-0.19
		*O-*OH	-1142.60	0.34	1.52
Ag-C		Slab	-1125.52	0	0
		*OH	-1137.31	0.33	-0.63
		*O	-1132.41	0.04	0.58
		*OOH	-1141.42	0.33	2.69
		*OH-*OH	-1147.96	0.59	-0.19
		*O-*OH	-1142.80	0.31	1.28

Table S14. Total energies (E), free energy corrections of surface-adsorbed molecules [$G(T) = E_{\text{ZPE}} + \Delta U - TS$], and Gibbs free energy (ΔG^*) of oxidation intermediates adsorbed on different coordinated metal sites in the Ni₂/h-BN system under the AEM and OCM mechanisms.

	Species	E (eV)	$G(T)$ (eV)	ΔG^* (eV)
Ni-B	Slab	-1119.94	0	0
	*OH	-1131.42	0.25	-0.40
	*O	-1127.08	0.06	0.35
	*OOH	-1135.54	0.31	2.97
	*OH-*OH	-1141.96	0.64	0.29
	*O-*OH	-1139.28	0.47	-0.61
Ni-N	Slab	-1119.94	0	0
	*OH	-1131.87	0.35	-0.76
	*O	-1127.08	0.06	0.35
	*OOH	-1136.10	0.36	2.46
	*OH-*OH	-1141.96	0.64	0.29
	*O-*OH	-1136.53	0.29	1.96

Table S15. Total energies (E), free energy corrections of surface-adsorbed molecules [$G(T) = E_{\text{ZPE}} + \Delta U - TS$], and Gibbs free energy (ΔG^*) of oxidation intermediates adsorbed on different coordinated metal sites in the Ru₂/h-BN system under the AEM and OCM mechanisms.

	Species	E (eV)	$G(T)$ (eV)	ΔG^* (eV)
Ru-B	Slab	-1125.78	0	0
	*OH	-1137.06	0.25	-0.19
	*O	-1132.74	0.03	0.50
	*OOH	-1140.76	0.31	3.60
	*OH-*OH	-1148.96	0.60	-0.90
	*O-*OH	-1144.39	0.36	0.02
Ru-N	Slab	-1125.78	0	0
	*OH	-1137.66	0.32	-0.72
	*O	-1134.05	0.05	-0.79
	*OOH	-1144.67	0.39	-0.23
	*OH-*OH	-1148.96	0.60	-0.90
	*O-*OH	-1145.20	0.32	-0.83

Table S16. Total energies (E), free energy corrections of surface-adsorbed molecules [$G(T) = E_{\text{ZPE}} + \Delta U - TS$], and Gibbs free energy (ΔG^*) of oxidation intermediates adsorbed on different coordinated metal sites in the Rh₂/h-BN system under the AEM and OCM mechanisms.

	Species	E (eV)	$G(T)$ (eV)	ΔG^* (eV)
Rh-B	Slab	-1123.94	0	0
	*OH	-1134.43	0.25	0.59
	*O	-1129.54	0.04	1.86
	*OOH	-1138.78	0.31	3.74
	*OH-*OH	-1145.54	0.60	0.67
	*O-*OH	-1142.23	0.43	0.41
Rh-N	Slab	-1123.94	0	0
	*OH	-1135.05	0.32	0.05
	*O	-1129.54	0.04	1.86
	*OOH	-1139.03	0.29	3.46
	*OH-*OH	-1145.54	0.60	0.67
	*O-*OH	-1141.07	0.32	1.45

Table S17. Total energies (E), free energy corrections of surface-adsorbed molecules [$G(T) = E_{\text{ZPE}} + \Delta U - TS$], and Gibbs free energy (ΔG^*) of oxidation intermediates adsorbed on different coordinated metal sites in the Pd₂/h-BN system under the AEM and OCM mechanisms.

		Species	E (eV)	$G(T)$ (eV)	ΔG^* (eV)
Pd-B		Slab	-1119.06	0	0
		*OH	-1130.87	0.34	-0.64
		*O	-1125.81	0.05	0.73
		*OOH	-1135.12	0.35	2.55
		*OH-*OH	-1141.56	0.66	-0.18
		*O-*OH	-	-	-
Pd-N		Slab	-1119.06	0	0
		*OH	-1130.87	0.33	-0.64
		*O	-1125.81	0.05	0.73
		*OOH	-1135.12	0.35	2.55
		*OH-*OH	-1141.56	0.66	-0.18
		*O-*OH	-	-	-

Table S18. Total energies (E), free energy corrections of surface-adsorbed molecules [$G(T) = E_{\text{ZPE}} + \Delta U - TS$], and Gibbs free energy (ΔG^*) of oxidation intermediates adsorbed on different coordinated metal sites in the $\text{Ag}_2/\text{h-BN}$ system under the AEM and OCM mechanisms.

	Species	E (eV)	$G(T)$ (eV)	ΔG^* (eV)
Ag-B	Slab	-1112.23	0	0
	*OH	-1123.50	0.32	-0.12
	*O	-1120.36	0.09	-0.62
	*OOH	-1127.04	0.32	3.76
	*OH-*OH	-1133.48	0.60	-0.18
	*O-*OH	-	-	-
Ag-N	Slab	-1112.23	0	0
	*OH	-1123.50	0.32	-0.12
	*O	-1118.23	0.05	1.47
	*OOH	-1127.55	0.34	3.27
	*OH-*OH	-1133.48	0.60	1.02
	*O-*OH	-	-	-

Table S19. Total energies (E), free energy corrections of surface-adsorbed molecules [$G(T) = E_{\text{ZPE}} + \Delta U - TS$], and Gibbs free energy (ΔG^*) of oxidation intermediates adsorbed on different coordinated metal sites in the M_2/Gra system under the AEM and OCM mechanisms.

	Species	E (eV)	$G(T)$ (eV)	ΔG (eV)
Fe-C	Slab	-1180.47	0	0
	*OH	-1192.36	0.28	-0.78
	*O	-1188.77	0.05	2.42
	*OOH	-1196.63	0.32	-0.82
	*OH-*OH	-1204.14	0.58	-1.42
	*O-*OH	-1199.39	0.32	-0.34
Co-C	Slab	-1178.71	0	0
	*OH	-1190.93	0.34	-1.04
	*O	-1185.61	0.04	0.57
	*OOH	-1195.14	0.34	2.18
	*OH-*OH	-1201.74	0.56	-0.79
	*O-*OH	-1196.89	0.34	0.43
Ni-C	Slab	-1174.81	0	0
	*OH	-1187.21	0.35	-1.21
	*O	-1182.75	0.06	-0.44
	*OOH	-1191.43	0.37	2.01
	*OH-*OH	-1197.54	0.60	-0.45
	*O-*OH	-1192.79	0.36	0.66
Cu-C	Slab	-1170.00	0	0
	*OH	-1181.12	0.34	0.04
	*O	-1176.41	0.05	1.07
	*OOH	-1185.35	0.34	3.26
	*OH-*OH	-1191.43	0.62	0.86
	*O-*OH	-1185.76	0.32	2.81
Ru-C	Slab	-1182.09	0	0
	*OH	-1193.89	0.28	-0.68
	*O	-1189.60	0.04	-0.03
	*OOH	-1198.17	0.32	2.51
	*OH-*OH	-1205.35	0.56	-1.03
	*O-*OH	-1201.07	0.32	-0.40
Rh-C	Slab	-1179.73	0	0
	*OH	-1191.53	0.33	-0.63
	*O	-1186.26	0.04	0.94
	*OOH	-1195.73	0.32	2.59
	*OH-*OH	-1201.97	0.53	-0.03
	*O-*OH	-1196.89	0.31	1.42
Pd-C	Slab	-1173.75	0	0

	*OH	-1185.96	0.34	-1.03
	*O	-1181.28	0.05	-0.05
	*OOH	-1190.15	0.36	2.22
	*OH-*OH	-1196.6	0.6	-0.56
	*O-*OH	-1191.2	0.3	1.12
Ag-C	Slab	-1165.93	0	0
	*OH	-1177.28	0.32	-0.20
	*O	-1172.32	0.04	1.08
	*OOH	-1181.45	0.32	3.06
	*OH-*OH	-1187.25	0.61	0.96
	*O-*OH	-1181.34	0.31	3.16

Table S20. Gibbs free energy of *O-*OH for M₂/h-BN. The sites highlighted in red correspond to the dehydrogenation positions.

	ΔG_{*O-*OH} (eV) of M-B	ΔG_{*O-*OH} (eV) of M-N
Ni	-0.61	1.96
Ru	0.02	-0.83
Rh	0.41	1.45

Table S21. Gibbs free energy of *O-*O for M₂/L(N), M₂/L(B), M₂/h-BN, and M₂/Gra.

	$\Delta G_{*O,*O}$ of M ₂ /L(N)	$\Delta G_{*O,*O}$ of M ₂ /L(B)	$\Delta G_{*O,*O}$ of M ₂ /h-BN	$\Delta G_{*O,*O}$ of M ₂ /Gra
Fe	1.63	-	-	1.87
Co	2.08	2.25	-	2.48
Ni	-	3.00	2.97	2.72
Cu	3.43	-	-	3.23
Zn	4.03	-	-	-
Ru	1.82	2.33	2.00	2.20
Rh	-	3.05	3.22	3.07
Pd	-	3.58	-	3.13
Ag	-	3.24	-	3.46